2

CONF-880122--12

HYDROGEN TURBINES FOR SPACE POWER SYSTEMS: A SIMPLIFIED AXIAL FLOW GAS TURBINE MODEL

SAND--87-1923C

DE88 009585

Steven L. Hudson

Advanced Power Systems Division

Sandia National Laboratories

P.O. Box 5800

Albuquerque, NM 87185

505-846-3070

ABSTRACT

This paper describes a relatively simple axial flow gas expansion turbine mass model, which we developed for use in our space power system studies. The model uses basic engineering principles and realistic physical properties, including gas conditions, power level, and material stresses, to provide reasonable and consistent estimates of turbine mass and size. Turbine design modifications caused by boundary layer interactions, stress concentrations, stage leakage, or bending and thermal stresses are not accounted for. The program runs on an IBM PC, uses little computer time and has been incorporated into our system-level space power platform analysis computer codes. Parametric design studies of hydrogen turbines using this model are presented for both nickel superalloy and carbon/carbon composite turbines. The effects of speed, pressure ratio, and power level on hydrogen turbine mass are shown and compared to a baseline case 100-MWe, 10,000-rpm hydrogen turbine. Comparison with more detailed hydrogen turbine designs indicates that our simplified model provides mass estimates that are within 25% of the ones provided by more complex calculations.

DISCLAIMER

HYDROGEN TURBINES FOR SPACE POWER SYSTEMS: A SIMPLIFIED AXIAL FLOW GAS TURBINE MODEL

Steven L. Hudson
Advanced Power Systems Division
Sandia National Laboratories
P.O. Box 5800
Albuquerque, NM 87185
505-846-3070

INTRODUCTION

The analysis of hydrogen-cooled, turbine-generator powered space weapon systems has resulted in the need for a relatively simple, but reasonably accurate hydrogen gas expansion turbine model. Such a simplified turbine model would require little computational time, provide reasonably accurate volume and mass estimates, and allow incorporation into system level computer programs. This model would then allow optimization studies to be performed on multiparameter space power systems for various operating conditions (Edenburn 1987) and provide improved turbine mass and size estimates when compared to empirical correlations or power law approaches. For these reasons we have developed an axial flow gas expansion turbine model that runs on an IBM PC and have used it during the past year as a comparative model in space power system studies at Sandia.

Using concepts from fluid dynamics, thermodynamics, and strength of materials, the turbine model determines: (1) the force on the rotating turbine blades caused by the momentum change of the turbine working fluid; (2) the energy transfer from the turbine working fluid to the rotating blades; (3) the flow area required by the working fluid as it passes through a turbine stage; and (4) the limiting stage blade speed due to centrifugal forces. This provides a realistic basis for the turbine model and allows a consistent comparison between turbines for most system design effects. The turbine model computes the maximum rotational speed, working fluid flow rate, outlet pressure, number of stages, individual turbine stage disk and blade sizes, and overall turbine mass. As such, the turbine model requires realistic input data. These input items include turbine power level, working fluid inlet conditions, required exit temperature, turbine material strength and density, and turbine internal design values (nozzle angle, aspect ratio, and work coefficient that are defined later). Optionally, speed and/or stage efficiency values may also be specified. Despite this required input data, the turbine model is considered simplified because it does not account for more detailed design considerations such as boundary layer effects, shock waves, stress concentrations, seal and tip leakage, three-dimensional flow effects, and bending and thermal stresses. These later limitations, although very real in determining the efficiency or capability of a given turbine design, generally only modify a basic turbine design and have minimal mass impact.

The principles of this turbine model apply to any gas or noncondensing vapor axial flow turbine. However, hydrogen turbines are discussed in this paper due to their importance to space burst power platforms and their meager design data available to date. The turbine model description, limitations, and results of typical parametric studies are presented in the following sections of this report.

TURBINE MODEL DEVELOPMENT AND EQUATIONS

The turbine model defines the turbine stage size in terms of stage blade length, disk radius, and turbine speed. Blade length and disk radius are considered because they are the primary size limiting dimensions of the turbine stage. The model calculates a stage mass based on these size criteria and sums the individual stage masses to give the complete turbine size and mass. However, the stage blade lengths, disk radii, and turbine speed are dependent on the stage work, stage outlet gas flow conditions, number of stages, and blade and disk material strengths and cannot be solved for explicitly. Thus, the equations must be iteratively solved. This section develops the equations that relate the basic turbine design variables to the above stage size criteria, while the following section indicates their sequence of solution.

Energy transfer occurs at each stage of an axial flow turbine when high velocity gas impacts the rotating blades. This fluid interaction imparts a force to the moving blades, thereby transmitting power to the turbine shaft and lowering the enthalpy of the gas. This two-dimensional flow condition (axial and tangential) is represented by the vector velocity diagram of

Figure 1 for a typical turbine stage with nozzle (stator) and blade (rotor). The gas flow enters the stage at absolute velocity c_1 and is accelerated through the nozzles to absolute velocity c_2. This higher velocity gas flow then impinges on the rotor blades, does work, and leaves the stage at absolute velocity c_3. The force on the turbine blades, caused by the change in absolute tangential velocity ($c_{2z} - c_{3z}$) of the gas flow, moves the blades at a mean stage blade speed of U_s. Application of the fluid impulse-momentum principle allows calculation of the stage work per unit mass of working fluid, W_s, as:

$$W_s = (c_{2z} - c_{3z})(U_s). \qquad \text{Eq. 1}$$

Note from Figure 1 that the outlet tangential velocity, c_{3z}, is typically opposite in direction and therefore negative relative to c_{2z}. Thus, the stage work, W_s, is always a positive quantity. A stage work coefficient, ψ, can be defined as (Wilson, 1984):

$$\psi = (c_{2z} - c_{3z})/U_s. \qquad \text{Eq. 2}$$

Equation 2 reveals that the stage work coefficient is simply the ratio of change in gas tangential velocity to the mean stage blade speed. A work coefficient of one occurs when the tangential velocity c_{2z} nearly equals U_s and results in the stage leaving gas velocity, c_3, being nearly axial. This condition generally provides maximum stage efficiency because of low relative (to the blade) velocities. Higher tangential velocities result in higher work coefficients and generally lower stage efficiencies. However, the higher velocities are limited

to the sonic gas velocity unless the turbine stage is designed to accommodate these supersonic flows.

From Equations 1 and 2 it can be seen that the turbine stage work is:

$$W_s = (\psi)(U_s^2). \qquad \text{Eq. 3}$$

Although the stage work coefficient is an input parameter selected by the turbine designer, the stage work can be determined only after the stage blade speed is known. This blade speed, U_s, is the speed of the blade at the stage mean radius, R_m, and is related to the turbine angular speed in radians/sec, N, by:

$$U_s = R_m N. \qquad \text{Eq. 4}$$

R_m varies with the stage blade length, L_s, and disk radius, R_d, since $R_m = R_d + L_s/2$, and is not known a priori for each stage of a turbine design. Stage blade speed must be obtained from a knowledge of the working fluid mass flow, the required stage outlet flow area, and the blade and disk specific strengths.

The mass flow rate through the turbine, m, is calculated from the specified (1) turbine design power, W_t; (2) turbine inlet temperature, T_i; (3) turbine outlet temperature, T_o; and (4) working fluid average specific heat, c_{pave}, by:

$$m = W_t/[c_{pave}(T_i - T_o)]. \qquad \text{Eq. 5}$$

Since specific heat is a function of temperature, c_{pave} is the average working fluid specific heat between T_i and T_o. c_p for hydrogen has little variation with pressure for temperatures greater than 300 K, so pressure effects on c_p are not included.

Stage outlet flow area is calculated by application of the conservation of mass (continuity) through the turbine stage and by realizing that the mass flow, m, is constant. Since velocity equals volume flow rate divided by flow area, two-dimensional flow through the turbine stage results in:

$$c_{3x} = m\, v_3/(2\pi R_m L_s) \qquad \text{Eq. 6}$$

where c_{3x} is the stage outlet axial velocity, v_3 is the specific volume of the outlet gas, and the quantity $2\pi R_m L_s$ is the outlet flow annulus area. The assumption of ideal gas behavior for gas flow through each stage of the turbine allows a simple determination of the outlet gas specific volume from stage outlet static pressure, P_3, and static temperature, T_3. However, quantifying c_{3x} requires imposing two restrictions on the turbine stage design in order to limit the required stage input design data. First, restriction to a 50% reaction stage provides for equal enthalpy drop across rotor and stator and requires that the blade inlet absolute velocity, c_2, equals the blade outlet relative velocity, w_3 (see Figure 1). Second, restriction to constant axial velocity throughout the turbine stage requires that c_{2x} equals c_{3x}. These restrictions, which are common design practice in the gas turbine industry, do not limit or bias our turbine model. However, they result in geometric similarity for Figure 1 and require angles a_2 and b_3 to be equal and angles b_2 and a_3 to be equal. Thus:

$$c_{2z} = U_s - c_{3z} \qquad \text{Eq. 7}$$

and;

$$\psi = (2c_{2z} - U_s)/U_s \qquad \text{Eq. 8}$$

Also, $c_{2z} = c_2 \sin(a_2)$ and $c_2 = c_{2x}/\cos(a_2)$ so:

$$c_{2x} = c_{3x} = (\psi U_s + U_s)/(2\tan[a_2]) \qquad \text{Eq. 9}$$

Equation 9 expresses the stage outlet axial velocity as a function of only two turbine input design parameters, ψ and the nozzle-to-blade angle, a_2. Finally, Equations 4, 6, and 9 are combined to yield the final form of the stage continuity equation:

$$m\ R\ T_3 \tan(a_2) = \pi\ P_3\ (\psi+1)\ R_m^2\ N\ L_s \qquad \text{Eq. 10}$$

which specifies the relationship between turbine speed, stage blade length, mean stage radius, stage outlet gas conditions, and input turbine design parameters. R is the gas constant for the particular turbine working fluid.

The turbine stage outlet temperature for use in equation 10 is determined by applying the first law of thermodynamics (conservation of energy) between the inlet and outlet of each turbine stage. For adiabatic steady flow and no change in potential energy, the first law for a unit mass of gas results in:

$$h_3 = h_1 - W_s + \frac{c_1^2 - c_3^2}{2} \qquad \text{Eq. 11}$$

where h_3 is the outlet gas static enthalpy and h_1 is the stage inlet gas static enthalpy. For an ideal gas enthalpy is a function of temperature only so equation 11 becomes:

$$T_3 = T_1 - W_s/c_p + \frac{c_1^2 - c_3^2}{2c_p} \qquad \text{Eq. 12}$$

The stage inlet static temperature, T_1, and inlet velocity, c_1, are known from the previous stage. However, c_3 must be determined from the geometry of the similar velocity triangles of

Figure 1. From the previous restrictions of 50% reaction stages and constant axial velocity, it can be shown from the blade inlet and exit velocity triangle geometry that:

$$c_3=U_s[\{(\psi-1)/2\}^2+\{(\psi+1)/(2\tan[a_2])\}^2]^{1/2}. \quad \text{Eq. 13}$$

Thus, the stage outlet velocity depends only on stage blade speed, work coefficient, and nozzle-to-blade angle.

The stage outlet static pressure for use in Equation 10, P_3, is related to the stage efficiency and stage inlet and outlet temperatures. From Figure 2, the turbine stage efficiency, n_s, is (Horlock 1966):

$$n_s = (T_{t1} - T_{t3})/(T_{t1} - T_{t3s}) \quad \text{Eq. 14}$$

for a constant specific heat across the stage. Equation 14 defines the total-to-total stage efficiency and uses total rather than static thermodynamic properties. The subscript "t" represents total temperatures and for an ideal gas is:

$$T_t = T + c^2/(2c_p). \quad \text{Eq. 15}$$

The turbine stage efficiency is based on an isentropic expansion from the stage inlet total pressure, P_{t1}, to the stage outlet total pressure, P_{t3}. T_{t3s} in Equation 14 is the stage outlet total temperature for this isentropic process. With constant specific heats for the temperature range of the turbine stage, the total inlet and outlet temperatures and pressures are related for this isentropic process by:

$$T_{t3s}/T_{t1} = (P_{t3}/P_{t1})^{k-1/k} \quad \text{Eq. 16}$$

where k is the ratio of gas specific heats (c_p/c_v). Further, the stage outlet total temperature, T_{t3}, is the temperature that results from the reversible adiabatic deceleration of the

outlet flowing gas to zero velocity (Jones and Hawkins 1960). Thus:

$$T_{t3}/T_3 = (P_{t3}/P_3)^{k-1/k}, \qquad \text{Eq. 17}$$

and similarly

$$T_{t1}/T_1 = (P_{t1}/P_1)^{k-1/k}. \qquad \text{Eq. 18}$$

Static pressures are represented in Figure 2 by the dotted constant pressure lines. Combining the above equations and solving for the stage outlet static pressure yields:

$$P_3 = P_1 \left[\frac{T_3 T_{1t}}{T_1 T_{3t}} - \frac{W_s T_3}{c_p n_s T_1 T_{3t}} \right]^{k/(k-1)}. \qquad \text{Eq. 19}$$

The turbine stage efficiency is specified by the program user or is determined within the program as a default value. We developed the turbine stage efficiency default values from empirical data available for large noncondensing steam turbine designs (Lapina 1983, Budenholzer 1970, Baumeister 1967, and Sorensen 1951). These stage efficiencies are represented in Figure 3 as functions of work coefficient and nozzle-to-blade angle. We based our default efficiency values on large reaction staged steam turbines because they have minimal performance losses when compared to their throughput with correspondingly high stage efficiencies. We consider these stage efficiencies to be nearly the highest stage efficiencies possible for any turbine design. The stage efficiencies in Figure 3 are total-to-total stage efficiencies and are intended to account for wall friction, eddy current, turbulence, and leakage losses. These efficiencies are only used as default values in the turbine design computer program and may be superseded by a user input value that accounts for lower performance or unique gas conditions. We

treat the stage efficiency as a constant throughout the turbine.

Equation 10 relates fluid conditions and turbine design criteria to the turbine size parameters of stage blade length, mean stage radius, and rotational speed. However, the stage blade length and radius are also limited in size by material stresses caused by speed induced centrifugal forces. Thus, the blade stress is (Horlock 1966):

$$b_{ss} = (T_f)(N^2)(R_m)(L_s) \qquad \text{Eq. 20}$$

where b_{ss} is the blade specific stress or ratio of material stress to density and T_f is a blade taper factor that relates the maximum tensile blade stress due to centrifugal loading of a straight blade to the blade stress associated with a tapered (reduced cross-sectional area from root to tip) blade. Equation 20 relates the blade stress to only pure tension centrifugal loadings and is maximum at the blade root. Aerodynamic or other induced bending stresses are not accounted for. T_f is kept at 0.7 in the computer calculations (Horlock 1966 and Sorensen 1951).

The corresponding disk stress, also caused by centrifugal forces, can be simplified to (Roark and Young 1975):

$$d_{ss} = 0.9(N^2)(R_m - L_s/2)^2 \qquad \text{Eq. 21}$$

where d_{ss} is the disk material specific stress. This relation is based on center-bored rotating disks of uniform thickness, no radial loading, and isotropic materials with Poisson's ratio of 0.33. Equation 21 calculates the maximum (tangential) stress existing within the disk, which occurs at the inner circumference of the bored disk. Although tapered disks may reduce this stress

level by 10 to 20 percent, circumferential loading due to the attachment of blades to the disk perimeter, would tend to negate this stress reduction. We therefore did not adjust the turbine design disk stress for these effects in our model. The material stresses calculated from Equations 20 and 21 are limited within the program so as not to exceed the user's input design material strengths. These input material strengths are based on creep strength properties and are dependent on the turbine operating time and temperature.

MODEL DESCRIPTION AND METHODOLOGY

The input design data for the turbine program can be separated into required inputs, optional inputs, and turbine internal design parameters. Required data inputs are inlet pressure, inlet temperature, turbine power output, outlet temperature (which may be an estimate based on expected turbine efficiency and pressure ratio), blade specific strength, disk specific strength, and material density. Optional data inputs include maximum turbine speed and stage efficiency. Normally, the calculated turbine speed within the program is the maximum speed possible that satisfies the input design criteria. If a lower turbine speed is specified by the user, then that speed is used for the subsequent turbine design. If stage efficiency is not specified, the program calculates a default value based on Figure 3. Finally, turbine internal design parameters include blade aspect ratio (used here as the ratio of blade length to blade axial thickness), nozzle-to-blade angle (angle a_2 in Figure 1), and work coefficient (Equation 2). If any of these

design parameters are not specified by the program user, default design values based on standard turbine design practice of 3, 70 degrees, and 2 are used by the program, respectively. Lower values of aspect ratio should be used for more brittle materials, higher blade loadings (because of high work coefficients or high gas density), or lower blade strength. Somewhat higher aspect ratios (4 to 5) should be expected for very long blades. Gases with high specific heats and sonic velocities, such as hydrogen and helium, should use turbine work coefficients greater than 2 (typically 4 or more).

From the input data, Equations 10, 20, and 21 are solved simultaneously within the program for the three unknowns of mean stage radius, stage blade length, and turbine speed. However, the values of stage outlet temperature and pressure for use in equation 10 are not directly known and must be determined iteratively. Thus, the computer program uses an iterative solution method, as shown by the flow chart in Figure 4, to determine the maximum speed turbine that meets the turbine input design criteria. If a lower speed is specified by the program user, then the program determines the minimum possible number of stages at this specified speed that does not exceed the allowable disk stress. Once the overall turbine outlet design conditions are satisfied, the individual stage dimensions are calculated. Additional program steps in the iteration process are shown in Figure 4.

In our model each stage of an axial flow turbine is separated into three distinct volumes with different average

densities. The overall turbine mass is then simply the sum of the masses of these identified volumes. The three stage volumes are (1) the turbine blade swept volume and associated nozzles; (2) the turbine disk volume; and (3) the void space between the stage disks. The turbine blade swept volume is the annular flow area multiplied by the stage length. The stage axial length, identified in Figure 5, is twice the stage blade length (to account for both blade and nozzle axial length) divided by the user-specified aspect ratio. The blade and nozzle volume are estimated to have a density of 30% of the user-specified input density in order to account for the blade and nozzle material. The turbine disk volume is treated as a solid uniform thickness disk with 100% of the density of the input value. Lastly, we treat the density of the interdisk volume as only 20% of the input density value in order to approximate the associated stage shaft and seal mass. Figure 5 is a cross section of a typical multistage axial flow turbine with these major components identified.

A casing mass is also determined for each stage of the turbine and included in the total turbine mass. This mass is calculated from the user-input material density and the wall thickness derived from hoop stress calculations and stage pressure.

Although there is no specific mass or volume allotted for some turbine mechanical components (such as bearings, shaft, inlet/outlet ducting, seals, or cooling passages), the gross density estimates of the various separate turbine volumes are intended to account for these items.

The turbine design program is valid for all working fluids that can be approximated as ideal gases. Further, a blade and disk cooling algorithm has been developed to study the effects on turbine size of increased material strengths due to lower component temperatures and the quantity of cooling gas required to maintain these lower component temperatures (Edenburn 1988).

MODEL LIMITATIONS

Although our gas turbine model provides reasonable size and mass constraints for many design options and gas conditions, we have found that a combination of certain design parameters may produce unrealistic results or conclusions. These potentially erroneous results include some combination of (1) a large number of stages; (2) very short blade lengths; or (3) low hub-to-tip radius ratios (the ratio of the flow annulus inner radius to the flow annulus outer radius).

A large number of stages generally result from using a hydrogen or helium working fluid with low stage work coefficients or low material strengths. For example, with work coefficients of about 2, a superalloy hydrogen turbine requires over 25 stages. This number of stages may cause shaft vibration or design problems that are not identified in our computer model. Presently, we size only each stage of a turbine and do not pass judgment within the program on the relative number of stages.

Very short blade lengths are considered to be less than 0.01 meter, although this is not a rigid criteria. These blade lengths are caused by a combination of low specified rotational speed, high disk material strength, and low power output. Thus,

for a given working fluid mass flow, only a small annulus flow area is required with a corresponding small blade length. The main concern with these shorter blade lengths is that the default stage efficiency values within the program are too high. Reduced efficiency will be caused by boundary-layer interactions and an increased fraction of gas leakage across the stage. Appropriate reductions in the stage efficiency by the user can account for this effect and provide reasonably accurate turbine designs.

Low hub-to-tip radius ratios are caused by excessively high expansions or pressure ratios through the turbine. Thus, the latter stages require a large flow area for a constant axial velocity design. This results in long stage blade lengths and low hub-to-tip radius ratios. Problems occur because the radial variation in blade speed differs significantly from the blade speed at the mean radius. For example, to obtain equal enthalpy drops of the gas passing through a turbine stage, the degree of reaction must decrease as you approach the hub or blade root from the mean radius. When the degree of reaction reaches zero, the stage acts as an impulse turbine at that radial location. Further reductions in reaction are then not possible and locations at lower radii than this point cause the gas to be recompressed or cause other design criteria in the model to be voided. The limiting hub-to-tip radius ratio in our model is determined from our requirement of 50% reaction at the mean blade radius. This results in a minimum hub-to-tip ratio of 0.547. Erroneous turbine designs result if lower hub-to-tip ratios occur for any stage.

Our turbine model approximates the final turbine mass from gross estimates of density for various regions of the turbine volume. These density estimates may not be appropriate for the various turbine materials that may actually be used. For example, carbon-carbon composite disks and blades may be attached to a superalloy shaft. Our model does not account for different material densities within the turbine. Also, we do not identify specifc components (other than blades, disks, and casing) within the turbine and do not provide specific mass estimates for these unidentified components. Thus, relatively massive items, such as bearings or shaft couplings, may not be adequately accounted for.

Finally, the thickness and corresponding mass of each turbine stage in our turbine model increases linearly with the user-specified aspect ratio, which is constant throughout the turbine. However, in reality shorter blades generally have lower aspect ratios, while longer blades have higher aspect ratios. Thus, in our model an average aspect ratio must be specified for reasonable mass results. This approximation may result in stages with short blade lengths having relatively thin disk thicknesses. This effect, coupled with a turbine design with many stages, may significantly underestimate the actual turbine volume and mass so we limit the minimum disk thickness for any stage to 0.01 meter.

It should be noted that the program user has an obvious effect on the program's calculated turbine mass by his selection of input parameters (as demonstrated by the Sandia turbine designs in Table 1). Thus, it is important that the user

understand the effect of the input parameters and adjust all parameters on a comparative and consistent basis. For example, shorter blades should be accompained by lower aspect ratios and lower stage efficiencies, while turbines with fewer stages should have their input material density increased to better account for bearings and casing inlet/outlet connections.

DESIGN COMPARISON

Table 1 compares results from Sandia's turbine model to a recent Garrett turbine design (Boyle and Riple 1987). This comparison is for carbon/carbon composite construction material, hydrogen gas, and 2000 K turbine inlet temperature. Other input parameters are as indicated in Table 1. Note that two sets of Sandia results are presented with differing aspect ratios, work coefficients, and nozzle-to-blade angles (a_2). The first calculation is for a more conventional nozzle angle of 70 degrees which results in an axial last stage gas velocity of 313 m/s. This nozzle angle requires longer blade lengths than for the Garrett design and has a correspondingly greater turbine volume and mass. The second Sandia calculation uses a nozzle-to-blade angle of only 51.6 degrees. This result approaches the Garrett stage blade lengths and flow area, but results in a last stage axial gas velocity of 676 m/s or more than twice that using Sandia's first set of input data. Although Sandia's second calculation results in significantly reduced mass, increased gas velocities and shorter blade lengths would require more careful manufacture to achieve the same stage efficiency as for Sandia's first calculation. This effect is also shown in Figure 3, where

Sandia's first and second sets of input data would have default stage efficiency values of nearly 92% and 83% respectively. However, the Garrett design and Sandia results show an overall turbine efficiency of 76% for the indicated gas temperatures and pressures, which requires a stage efficiency of only 72%.

The Sandia models result in the same number of stages and nearly the same first stage disk diameter as the Garrett design for the same limiting turbine speed and material stress. Further, Sandia's turbine masses, although somewhat different from each other, differ by only 25 per cent from Garrett's turbine mass.

PARAMETRIC STUDY RESULTS

We have used our turbine model to investigate the effects of rotational speed, pressure ratio, and power level on hydrogen turbine mass. As indicated in Figure 6, a nickel superalloy (material density of 8500 kg/m^3) turbine with 425-MPa disk material strength has a large variation in turbine mass due to changes in turbine design speed. For example, as design speed increases from 1000 rpm to 14,600 rpm for the 100-MWe turbine of Figure 6, turbine mass decreases by nearly two orders of magnitude. The increase in mass at lower rotational speeds is due to the increased disk radius at these lower speeds, which is caused by keeping the design disk stress at a constant value (since radius is inversely proportional to speed as shown by Equation 21). In addition, larger disk radii require shorter blades for a constant flow annulus with a resulting decrease in mean stage blade speed. Thus, lower turbine speeds also require

more stages (with a further mass increase). Turbine speed cannot be increased indefinitely, however, because blade strength finally limits the last stage blade lengths. For the superalloy turbine in Figure 6, this limit, which cannot be extrapolated, occurs at 14,600 rpm for blades with 425 MPa strength. The superalloy turbines in Figure 6 have an aspect ratio of 3, work coefficient of 4, and outlet temperature of about 800 K. The number of stages vary from 26 (high speed) up to 38 (1000 rpm) and the resulting turbine efficiencies are about 78%.

Figure 7 shows the further variation in hydrogen turbine mass with pressure ratio. For the same superalloy turbine design conditions as in Figure 6, turbine mass increases from about 430 kg at a pressure ratio of 1.5 to over 2000 kg at a pressure ratio of about 50. For the constant power output of 100 MWe, this equates to a specific mass of 0.0043 kg/kW to over 0.02 kg/kW. Turbine efficiency varies with pressure ratio (and number of stages) from about 70% at low pressure ratios to 78% at increased pressure ratios. The curves of Figure 7 also cannot be extrapolated since greater pressure ratios require longer last stage blades that soon reach their maximum allowable strength (at the stated turbine speed). This strength limit occurs even though the required gas flow to provide a given constant power decreases with increasing pressure ratios.

The effect of power level and inlet pressure for a hydrogen superalloy turbine is shown in Figure 8. Although higher pressures reduce turbine mass (by increasing the gas density), this effect is significant only at higher power levels. In fact,

the turbine mass at lower power levels is set by the disk diameter, which is dependent only on turbine speed. Thus, at lower power levels, turbine mass is nearly independent of gas pressure (the turbine casing thickness depends on gas pressure but is a small contribution to the overall turbine mass). Figure 8 again cannot be extrapolated since material strength limits still define the maximum possible turbine power output for the stated design conditions. For example, a 500-MWe nickel superalloy turbine operating at 6-MPa inlet pressure would have a maximum stress limited speed of only 7000 rpm with a resulting mass of over 6000 kg. The hydrogen turbine results of Figure 8 are based on a last stage blade allowable stress of 850 MPa and a stage work coefficient of 6. This results in less massive turbines than for the previous figures. The resulting turbine efficiencies are about 66%.

Figures 6 and 7 also show the effects of turbine rotational speed and pressure ratio on potential carbon-carbon composite hydrogen gas turbines. These curves are based on a mean material density of 3000 kg/m^3, blade aspect ratios of 2, and disk and blade stress limits of 450 MPa. The carbon-carbon turbine mass data of Figure 6 is based on a work coefficient of 3, while the curve in Figure 7 is for work coefficients ranging from 2 to 3. The lower work coefficients are used at pressure ratios less than about 40 with increasing work coefficients used at higher pressure ratios. This results in the carbon-carbon composite turbine from Figure 7 at a pressure ratio of 15 having a greater mass than the corresponding 10000 rpm turbine in Figure 6. At

pressure ratios less than 1.5 in Figure 7, turbine mass becomes nearly constant because of the increasing stage blade lengths due to the increased hydrogen flow rate.

CONCLUSIONS

A simplified gas expansion turbine computer model is available that runs on a portable computer yet requires very little computer time and can therefore be used in larger system codes. This model provides reasonable agreement with more detailed designs and allows parametric studies of turbine powered systems in a realistic and consistent manner. The model provides turbine size and mass based on material strengths, rotational speed, pressure ratio, power output, and gas properties.

Acknowledgments

This work was peformed at Sandia National Laboratories, which is operated for the U. S. Department of Energy under contract number DE-AC04-76DP00789, in support of the Independent Evaluation Group of the Strategic Defense Initiative's Space Power Office. Sandia is teamed with NASA Lewis Research Center for this support effort. The blade and disk cooling algorithm was developed by M. W. Edenburn of Sandia National Laboratories.

Table 1. 200 MWe Carbon/Carbon Composite Hydrogen Turbine Comparison

		Garrett Design	Sandia Model	
Input Parameters			1	2
Turbine Inlet Temp. (K)		2000		
Turbine Exhaust Temp. (K)		1500		
Turbine Inlet Press. (MPa)		3.446		
Design Stress (MPa)		690		
Turbine Speed (rpm)		10,000		
Blade Aspect Ratio		N/A[a]	2.0	1.5
Work Coefficient		N/A[a]	1.84	2.06
Nozzle Angle (degrees)		N/A[a]	70	51.6
Stage Efficiency (%)		N/A[a]	72	72
Output Parameters				
Turbine Pressure Ratio		5.0		
Turbine Efficiency (%)		76		
Number of Stages		14		
Disk Diameter (M)	First Stage:	0.973	0.965	0.965
	Last Stage:	0.58	0.965	0.965
Blade Length (M)	First Stage:	0.027	0.069	0.032
	Last Stage:	0.123	0.192	0.099
Turbine Length excluding bearings (M)		0.93	1.73	1.15
Turbine Mass (kg)		2300	2900	1680
Hydrogen Mass Flow (kg/sec)		25.7	24.1	24.1

a Not Available

References

Baumeister, T., ed. (1967) Standard Handbook for Mechanical Engineers, 7th edition, Mc-Graw Hill Book Company, New York.

Boyle, R.V. and J.C. Riple (1987) "Turbines in the Sky, The Power Behind Star Wars?," Mechanical Engineering, 109(7):38-45.

Budenholzer, R.A. (1970) "Turbine," in Encyclopaedia Britannica, W.E. Preece et al. eds., William Benton Publisher, Chicago, IL, Vol. 22, pp. 340-357.

Edenburn, M.W. (1987) "The Effect of Operating Temperature on Open, Multimegawatt Space Power Systems," in Trans. Fourth Symposium on Space Nuclear Power Systems, CONF-870102--Summs., held in Albuquerque, NM, 12-16 January 1987.

Edenburn, M.W. (1988) "The Effect of Operating Temperature and Turbine Blade Cooling on Brayton Cycle Space Power Systems," in Trans. Fifth Symposium on Space Nuclear Power Systems, CONF-880122--Summs., held in Albuquerque, NM, 11-14 January 1988.

Horlock, J.H. (1966) Axial Flow Turbines, Robert E. Krieger Publishing Co., Malabar, FL.

Jones, J.B. and G.A. Hawkins (1960) Engineering Thermodynamics, John Wiley & Sons, New York, pp. 506.

Lapina, R.P. (1983) "Calculator Method for Steam-Turbine Efficiency," Chemical Engineering, 90(13):37-42.

Roark, R.J. and W.C. Young (1975) Formulas for Stress and Strain, 5th ed., McGraw-Hill Book Co., New York, pp. 564-572.

Sorensen, H.A. (1951) Gas Turbines, Ronald Press Company, New York.

Wilson, D.G. (1984) The Design of High-Efficiency Turbomachinery and Gas Turbines, MIT Press, Cambridge, MA.

List of Figures

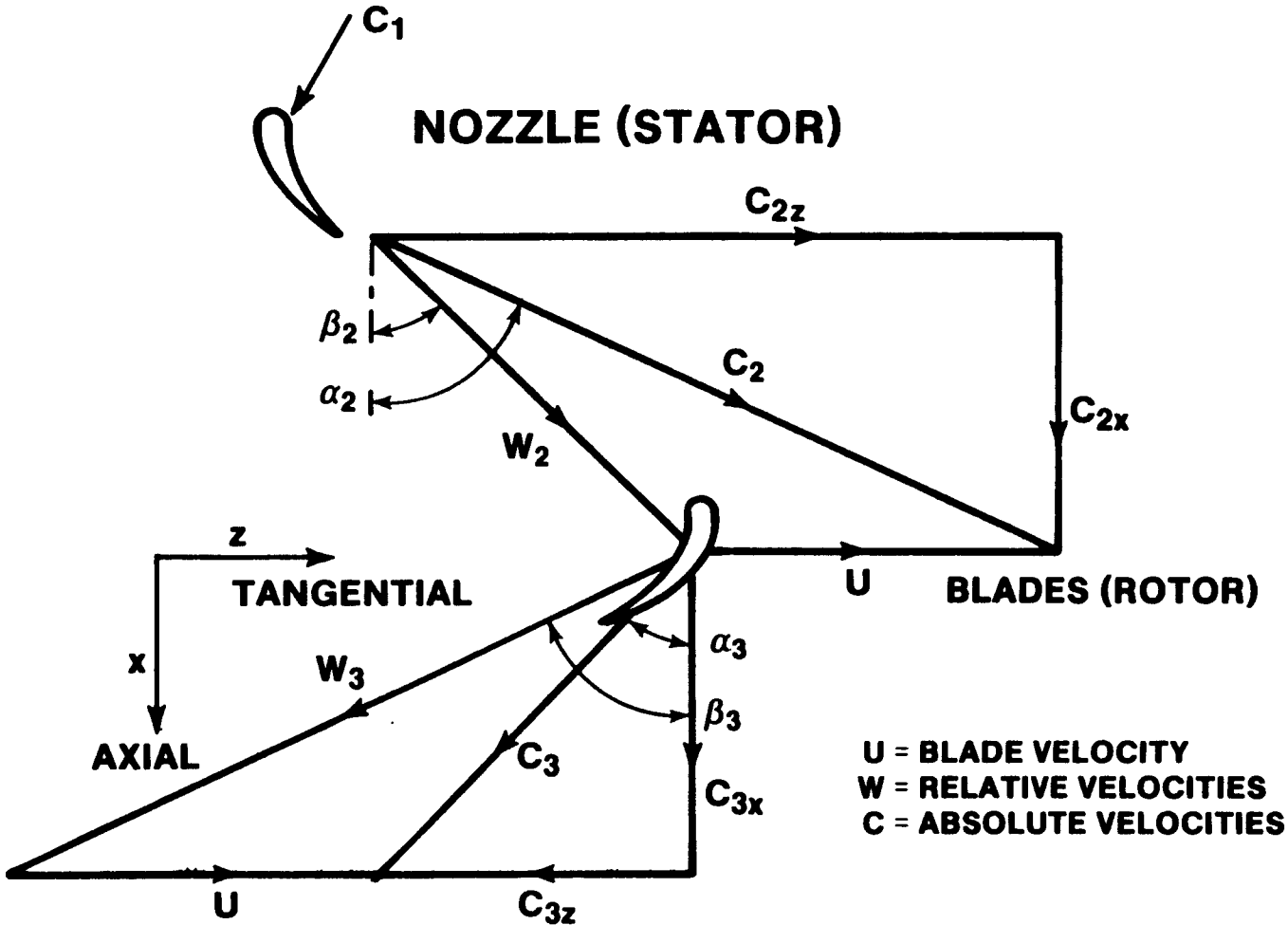
C1
NOZZLE (STATOR)
C2z
β2
α2
C2
C2x
W2
z
TANGENTIAL
U
BLADES (ROTOR)
x
AXIAL
W3
α3
β3
C3
C3x
U
C3z
U = BLADE VELOCITY
W = RELATIVE VELOCITIES
C = ABSOLUTE VELOCITIES

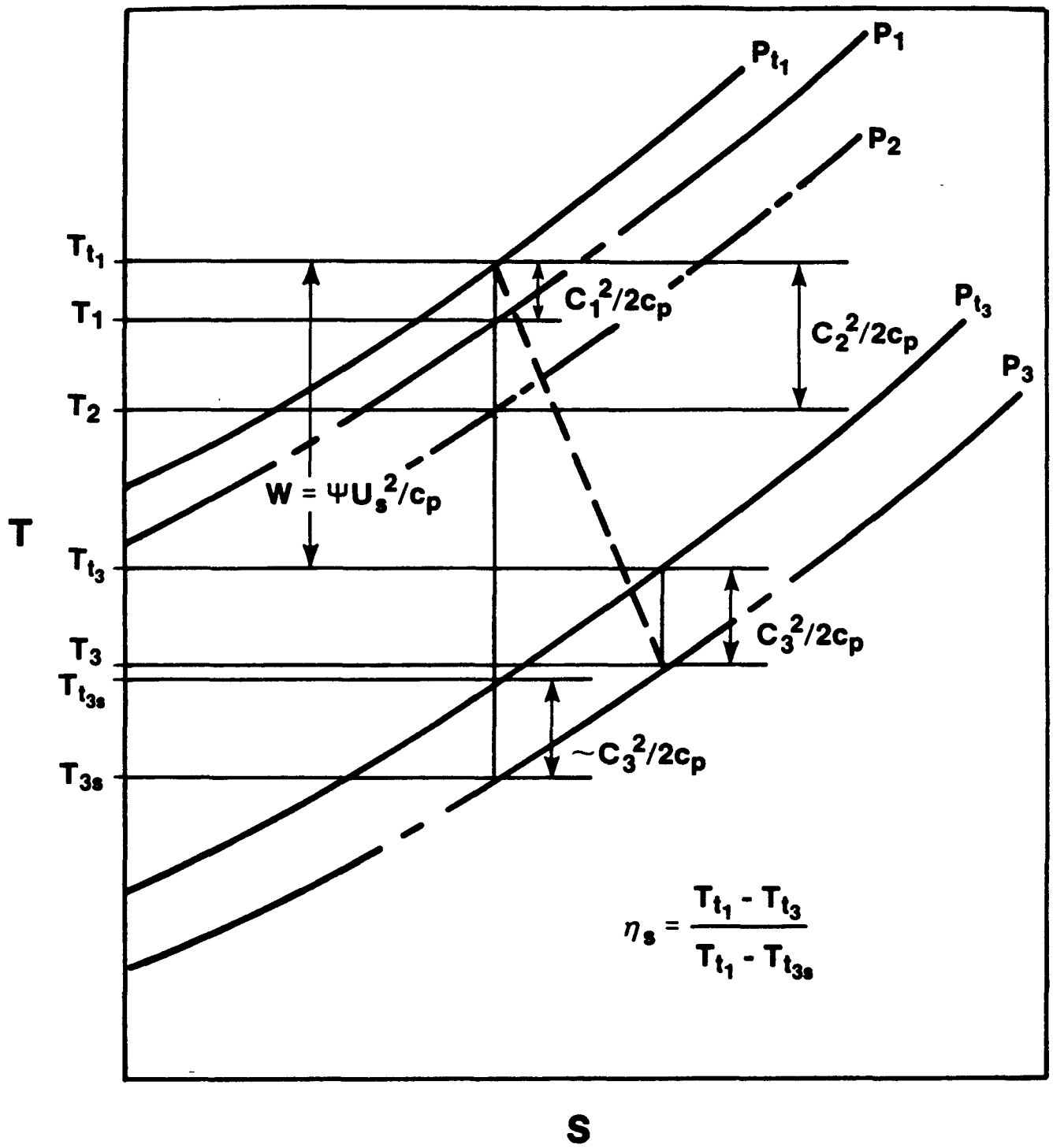
P_{t_1}
P_1
P_2
P_{t_3}
P_3
T_{t_1}
T_1
T_2
T_{t_3}
T_3
$T_{t_{3s}}$
T_{3s}
$C_1^2/2c_p$
$C_2^2/2c_p$
$C_3^2/2c_p$
$\sim C_3^2/2c_p$
$W = \Psi U_s^2/c_p$
T
S
$\eta_s = \frac{T_{t_1} - T_{t_3}}{T_{t_1} - T_{t_{3s}}}$

Figure 3. Turbine Model
Total-to-Total Stage Efficiency

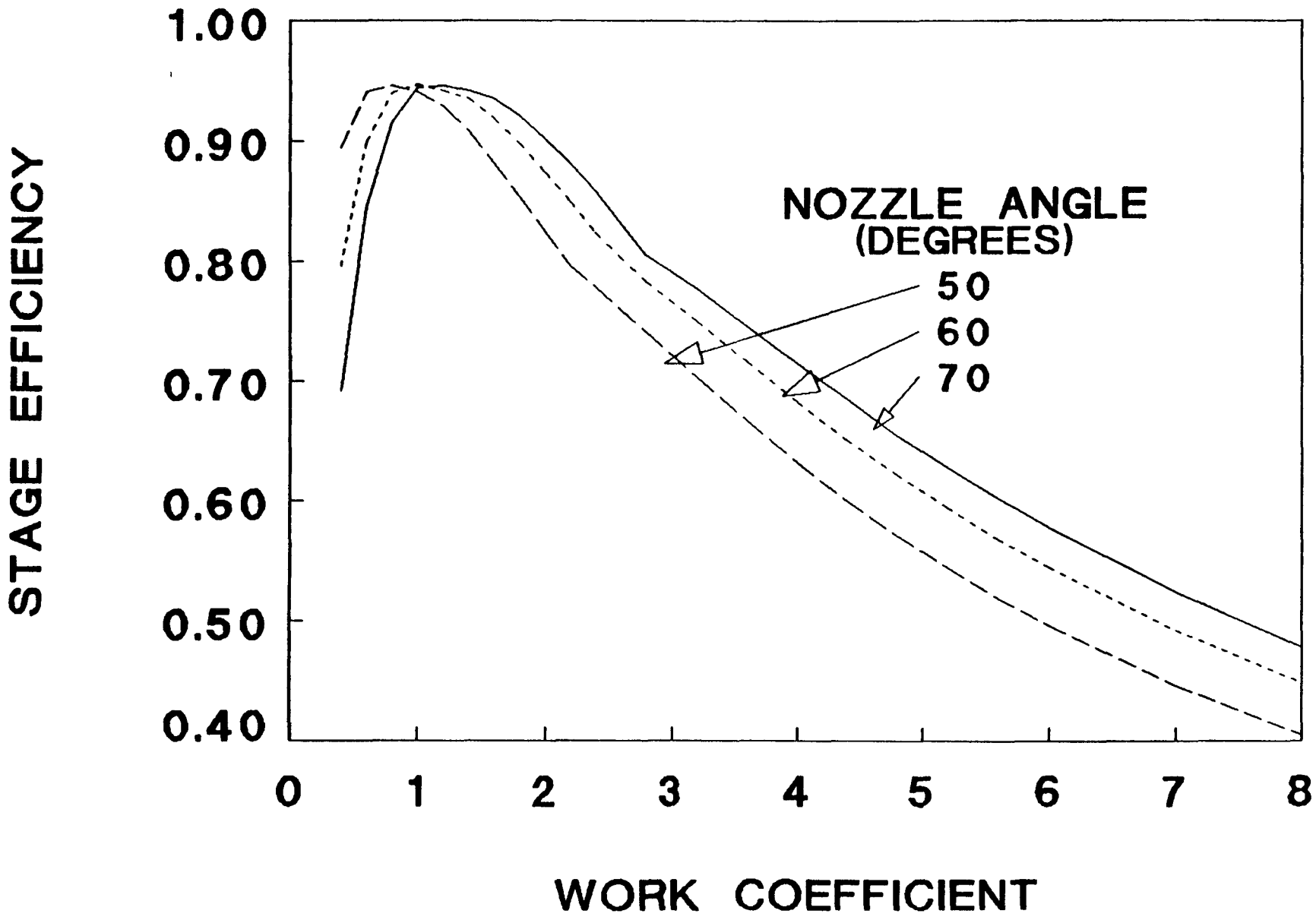

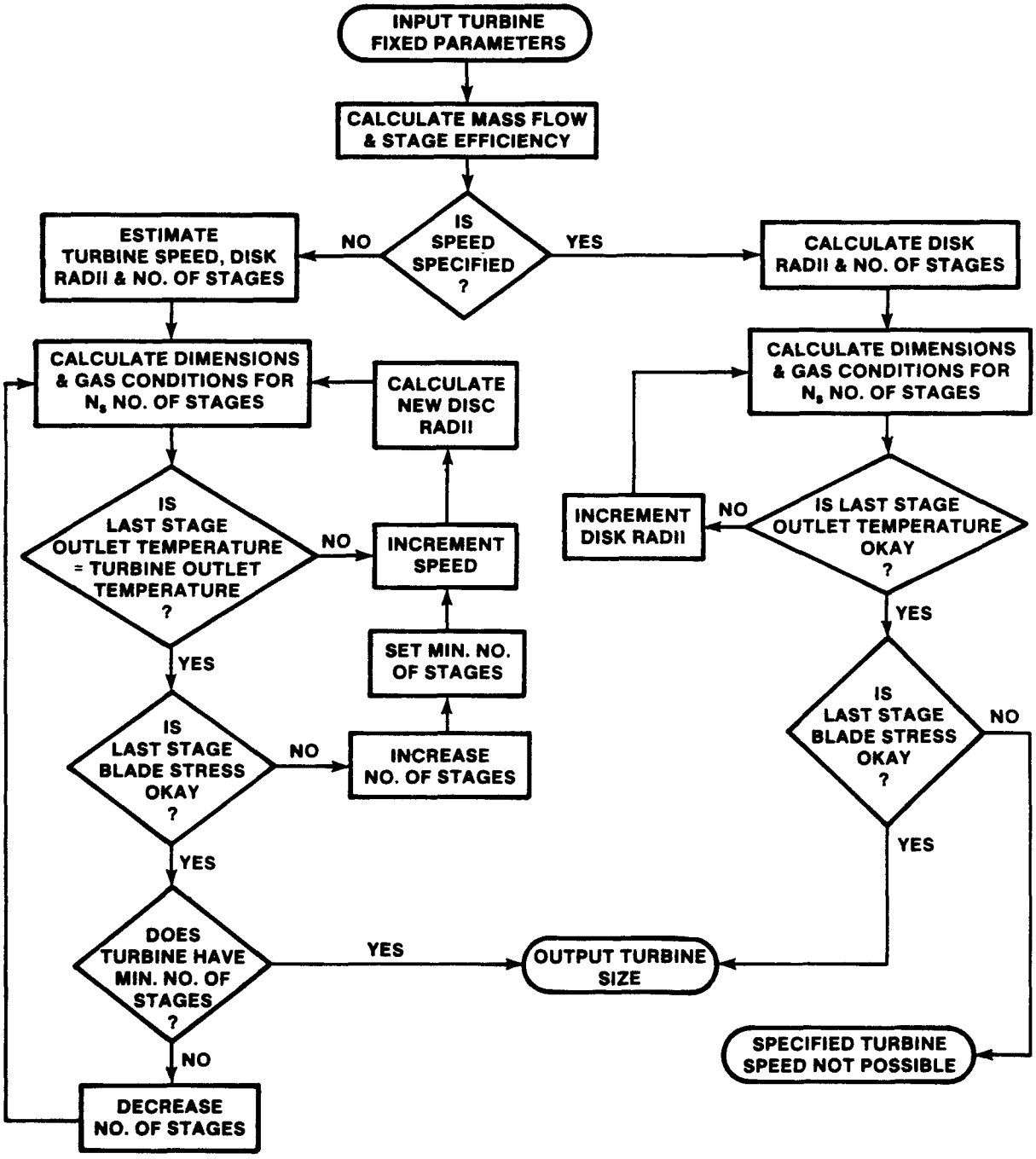
INPUT TURBINE FIXED PARAMETERS
CALCULATE MASS FLOW & STAGE EFFICIENCY
IS SPEED SPECIFIED ?
NO
YES
ESTIMATE TURBINE SPEED, DISK RADII & NO. OF STAGES
CALCULATE DISK RADII & NO. OF STAGES
CALCULATE DIMENSIONS & GAS CONDITIONS FOR N_s NO. OF STAGES
CALCULATE NEW DISC RADII
CALCULATE DIMENSIONS & GAS CONDITIONS FOR N_s NO. OF STAGES
IS LAST STAGE OUTLET TEMPERATURE = TURBINE OUTLET TEMPERATURE ?
NO
INCREMENT SPEED
INCREMENT DISK RADII
NO
IS LAST STAGE OUTLET TEMPERATURE OKAY ?
YES
YES
SET MIN. NO. OF STAGES
IS LAST STAGE BLADE STRESS OKAY ?
NO
INCREASE NO. OF STAGES
IS LAST STAGE BLADE STRESS OKAY ?
NO
YES
YES
DOES TURBINE HAVE MIN. NO. OF STAGES ?
YES
OUTPUT TURBINE SIZE
SPECIFIED TURBINE SPEED NOT POSSIBLE
NO
DECREASE NO. OF STAGES

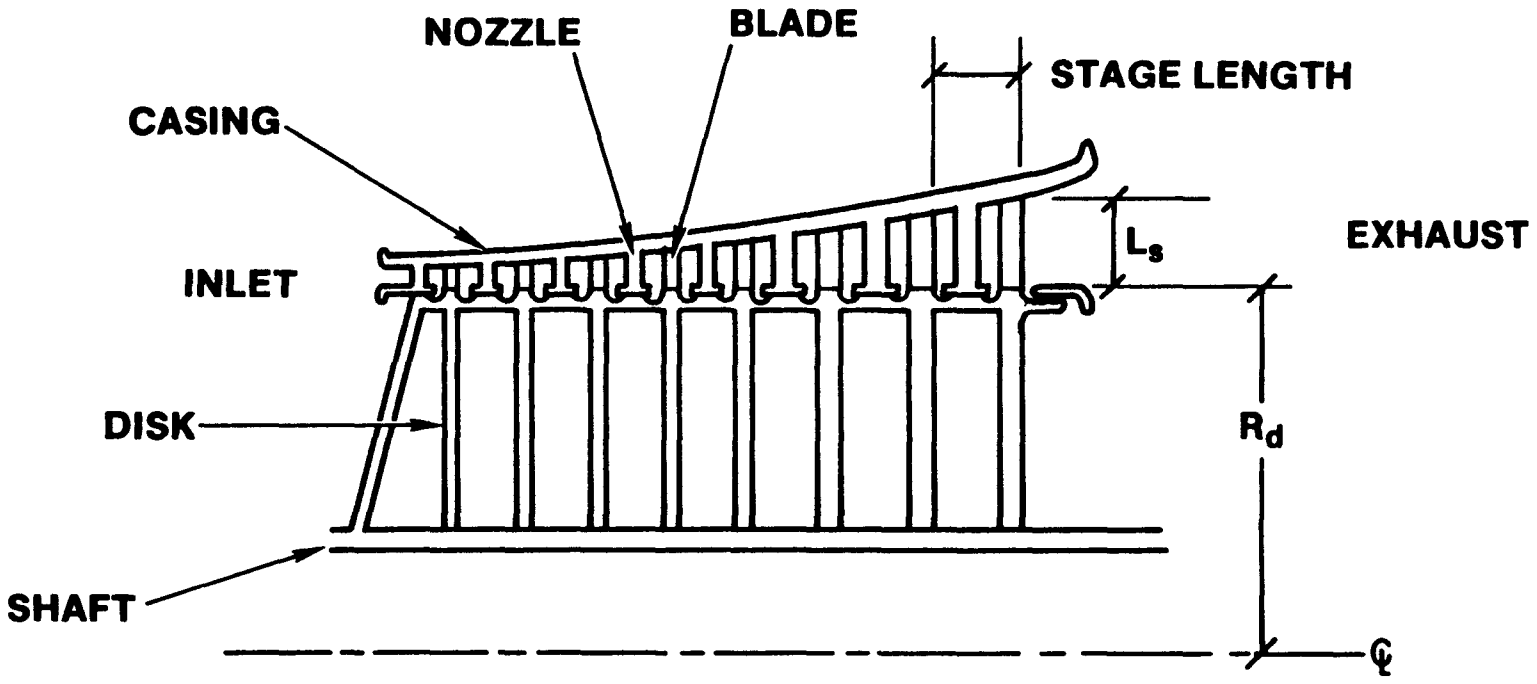
NOZZLE
BLADE
STAGE LENGTH
CASING
EXHAUST
INLET
L_s
DISK
R_d
SHAFT
℄

Figure 6. Variation in Hydrogen Turbine Mass with Rotational Speed

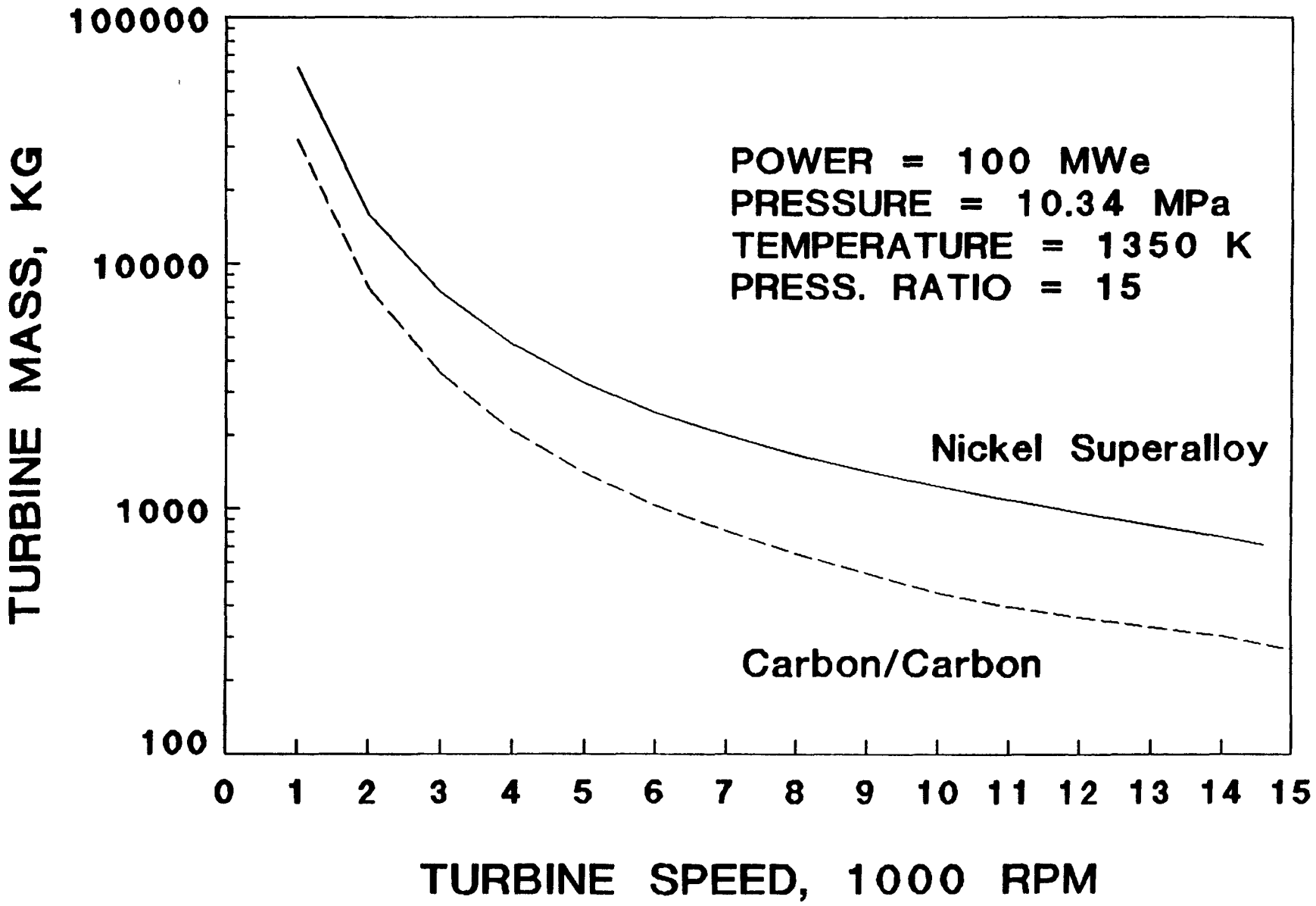

Figure 7. Variation of Hydrogen Turbine Mass with Pressure Ratio

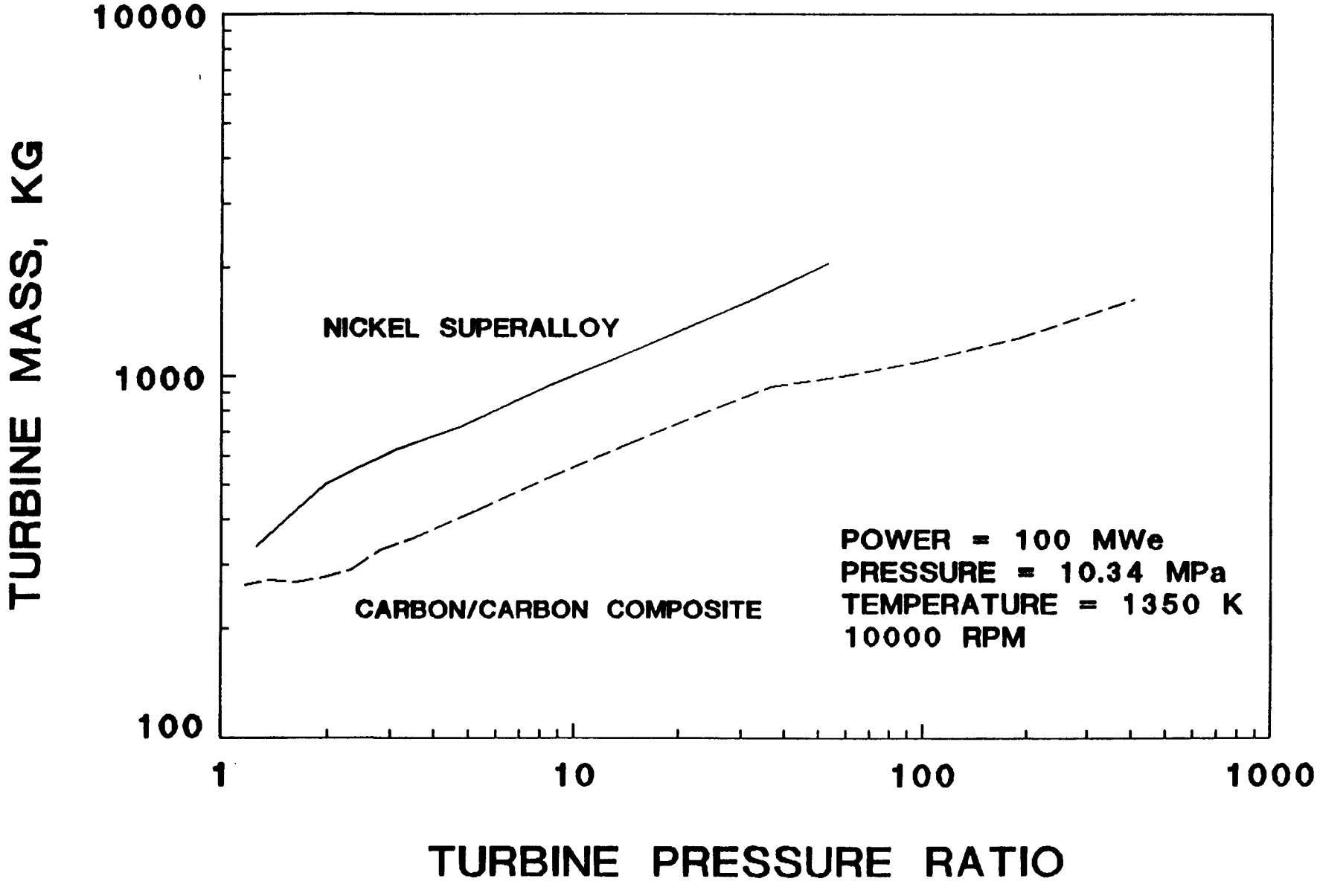

Figure 8. Effect of Power Level and Inlet Pressure on Hydrogen Turbine Mass